Optimal dynamic operation of natural gas combined cycles accounting for stresses in thick-walled components

Jairo Rúa[a],*, Roberto Agromayor[a], Magne Hillestad[b], Lars O. Nord[a]

[a] Department of Energy and Process Engineering, Norwegian University of Science and Technology, Trondheim, Norway
[b] Department of Chemical Engineering, Norwegian University of Science and Technology, Trondheim, Norway

HIGHLIGHTS

- Maximum gas turbine's load gradient is the main limitation during load changes.
- Gas turbine under-shooting compensates the steam cycle's slow transient.
- Proposed control methodology is able to predict stresses in thick-walled components.
- Stress monitoring allows optimal and safe control sequences under tight constraints.
- Suitability of the proposed methodology for start-up and shut-down applications.

ARTICLE INFO

ABSTRACT

Flexible natural gas combined cycles will play a fundamental role in future electric markets. Stresses in thick-walled components and gas turbine load ramps are arguably the main limiting factors during transient operation. Classical control strategies as PID are not suitable to incorporate technical constraints such as stress limits. This work presents a control methodology based on model predictive control where the stress in the walls of the high pressure drum and the first high pressure steam turbine rotor are computed simultaneously with the optimal control sequence. Thus, the maximum allowable stress in this equipment can be set as a constraint and the control actions imposed in the power plant ensure that these limits are not exceeded. Two cases simulating flexible operation under realistic conditions and tight constraints on the stress limits are included. Results show that with the proposed control methodology the natural gas combined cycle can respond to load step changes of 165 MW in 300 s, and can operate close to the material maximum stress limit without exceeding it. The robustness and flexibility of this methodology allows its application to different operation conditions such as start-ups and shut-downs.

1. Introduction

Anthropogenic greenhouse emissions have continuously increased since the industrial revolution. If this tendency is maintained, global warming is expected to reach temperatures of 1.5 °C above pre-industrial levels between 2030 and 2050 [1]. Power generation is the largest source of greenhouse gas emissions, mainly because of its reliance on fossil fuels [2]. Consequently, significant progress towards the Paris Agreement objectives of limiting the temperature increase to 2 °C above pre-industrial levels can be achieved in this sector if adequate measures are taken.

Electricity is progressively gaining relevance in the energy sector. It currently accounts for 20% of the final energy global consumption and

this amount is only expected to increase [3], reaching almost 40% in 2050 [4]. Therefore, the power generation system must undergone severe modifications in order to be able to produce more electricity while reducing its emissions. Renewable energy sources will play a major role in this new energy scenario and will have large shares in the electricity mix, predicted to reach about 40% of the power generation in 2040 [3]. Nevertheless, traditional thermal power plants will remain the largest source of electricity production [3].

In this context of increasing power generation from renewable energy sources, flexibility is and will be the foundation of a reliable and efficient electric system [3–8]. The lack of dispatchability of some renewable energy sources, mainly wind and solar, requires the existence of power generation alternatives that always allow to meet the power

* Corresponding author.
  E-mail addresses: jairo.r.pazos@ntnu.no (J. Rúa), lars.nord@ntnu.no (L.O. Nord).

Nomenclature

Latin Symbols

A	System of equations matrix [–]
a	Coefficients of the responses [–]
B	System of equations vector [–]
b	Coefficients of the manipulated variables [–]
C	Specific heat capacity [J/kg K]
c	Validity function centre [–]
d	Optimization weight vector [–]
E	Young's Modulus [MPa]
e	Stochastic error [–]
h	Convection coefficient [W/m^{2}K]
k	Heat conduction coefficient [W/m K]
M	Number of local models [–]
N	Time horizon [–]
n	Number of discretizations or variables [–]
p	Pressure [bar]
Q	Optimization weight matrix [–]
r	Radius [m]
T	Temperature deviation from design [K]
t	Time [s]
U	Manipulated variable [–]
u	Displacement [m]
w	Validity function width [–]
X	System of equations solution vector [–]
$\hat{y}$	Response [–]
z	Vector of optimization variables [–]

Greek Symbols

α	Thermal diffusivity [m^2/s]
α^*	Thermal expansion coefficient [1/K]
Δx	Space discretization size [m]
γ	Current operation point [–]
κ	Current measurement vector [–]
λ	Objective function weights [–]
ω	Rotational speed [rad/s]
ρ	Density [kg/m^3]
σ	Stress [MPa]
θ	Vector of coefficients [–]
υ	Poisson's ratio [–]
ξ	Validity function [–]

Subscripts

θ	Tangential direction
0	Initial conditions
drum	High-pressure drum
eq	Equality
eql	Linearised equivalent stress
i	Inner radius
ineq	Inequality
LMN	Local model network
m	Metal
o	Outer radius
r	Radial direction
rotor	First-stage steam turbine rotor
U	Past manipulated variables
y	Past responses
z	Longitudinal direction

Superscripts

high	Higher bound
low	Lower bound

demand [9]. Energy storage is considered as a promising technology supporting decarbonisation [10], but its application in a growing electricity market in the short- and mid-term is highly limited by its cost-effectiveness, technology maturity and commercial availability at large scale. Therefore, flexible operation of thermal power plants may be arguably considered as the main complement for renewable electricity production.

In the future European energy market, high renewable penetration will significantly increase the cycling operation of thermal power plants [11]. Modern gas-fired power plants are faster, less polluting and more efficient than coal-fired units at both full and minimum complaint load [12]. Thus, and despite of their utilization as based-load units, coal power plants will be less competitive because of the increase in both coal prices and CO_2 taxes, and due to their lack of flexibility and low part-load efficiency. On the contrary, the high efficiency of natural gas combined cycles at part-loads and their capability to face the fast cycling of renewables will lead to an increase of their share in the future European electricity market [11].

Operational flexibility in thermal power plants is normally assessed by three criteria: mimimun complaint load, start-up time and maximum load gradient [13]. The minimum complaint load of a natural gas combined cycle depends mainly on the gas turbine, as stable combustion and acceptable emissions limits must be guaranteed. Modern heavy duty gas turbines may offer a minimum load of 40–50% of the full load, but this level is expected to decrease to 30% [12,13]. In addition, if the power plant is expected to operate for long periods at low loads, the steam cycle design may be adapted to these conditions in order to increase the overall efficiency at part-load [14]. Start-up time and load gradients are influenced by the size of the equipment and the control

strategy imposed on the system. Bulk components with high heat capacity store large amounts of energy for long periods of time and hence prolong the transient of thermal power plants, leading to slow start ups and low ramp rates. Optimal design of flexible natural gas combined cycles must address this limitation, leading to power cycles where both high efficiency and fast response are achieved. Once the power plant is designed, the implemented control determines its adequate dynamic operation aiming at reducing the transient while ensuring safe and efficient operation.

Thermal stresses in thick-walled components are the primary limiting factor in the combined cycle transient as they may reduce its expected lifetime due to creep and fatigue. Therefore, proper control strategies may reduce the start-up time and increase the load gradient without exceeding the safety limit of the materials. Traditional control strategies in thermal power plants rely on PID controllers whose objective is fast system stabilization. Alobaid et al. [15] showed that start-up times can be halved without lost of stability if the gas turbine load gradient is increased and proper control of temperatures, pressures and levels is imposed on the power plant. However, material stresses were not assessed and hence it could not be verified whether this approach can be implemented in a real unit. Kim et al. [16] analysed the thermal stress development in the steam drum of a heat-recovery steam generator under three different start-up strategies. Results showed that the selection of the wrong approach and bad operational control may lead to excessive stresses that deteriorate the equipment. Can Gülen and Kim analyzed the stresses in the rotor and high-pressure drum of a natural gas combined cycle, showing the limitations they impose during the start-up and how appropriate control routines are required to avoid damaging this equipment [17]. Improvements in boiler's start-ups can

also be achieved with suitable temperature and mass flow control [18–20].

Optimization of dynamic operation can further improve the transient performance of thermal power plants. In this approach, both start-up and load gradient are treated as dynamic optimization problems [21]. Heuristic rules may be included in this type of control strategies to reduce the computational power required [22,23], but the strength of numerical optimization is partially lost by introducing experience-based constraints. Optimal start-up sequences that do not exceed the stress limits of critical components can be computed with this approach [24,25]. Casella and Petrolani [26] proposed two strategies to reduce the start-up time or the maximum peak stress of a three-pressure combined cycle with reheat. However, these strategies cannot be considered as optimal since no dynamic optimization was utilized. Optimal load gradient profiles can also be computed, ensuring that power is varied as fast as possible without violating the imposed constraints [27].

Model predictive control (MPC) enhances the strong capabilities of dynamic optimization. In this control methodology, a dynamic optimization problem that computes the optimal control sequence over a time horizon is solved at each control step. The first control action is subsequently implemented in the power plant. Thus, optimal control actions ensuring that the operational limits are not exceeded are always imposed. Prasad et al. [28,29] and Peng et al. [30,31] implemented an MPC algorithm to limit and control the superheated and reheated steam temperatures and the steam pressure in thermal power plants, obtaining faster behaviour of the system than with traditional PID controllers. A similar approach was followed by Lu and Hogg [32], who utilized an MPC to control the drum level, the steam pressure and the power generated by a thermal power plant. Model predictive control was also tested in industrial applications, leading to improvements over traditional approaches without exceeding the maximum allowable stresses in critical components [33]. Sindareh-Esfahani et al. [34] utilized model predictive control to improve the start-up of a power plant and impose constraints that limit the deterioration of the equipment. However, these constraints were imposed on the temperature gradients in critical components and not on the stress in their walls, which is the variable related to material deterioration and the actual limiting factor. Therefore, sub-optimal load ramps may be expected from this methodology.

As thermal and mechanical stresses in thick-walled equipment of thermal power plants are the main responsible of creep and fatigue [17,35–38], conservative control strategies are traditionally implemented in these power plants. To overcome this limitation, the stresses arising in sensitive components must be considered by the control strategy. Traditional approaches such as PID controllers do not allow to incorporate stress estimation and hence optimization-based strategies are required to impose constraints on these variables. This work proposes the first control methodology, based on MPC, that determines the optimal load ramp rates in the gas turbine whilst computes both mechanical and thermal stresses in critical components and imposes constraints on them at every control step. This control methodology ensures that the fastest load changes are achieved without exceeding the maximum allowable stress in the material of the equipment and the maximum load gradient in the gas turbine.

The different models used to develop the proposed control methodology and to test its application in a thermal power plant are described in Section 2. This includes the high-fidelity dynamic model of the NGCC that replicates the operation of a real power plant, and the stress and simplified models embedded in the optimization problem of the MPC that predict, respectively, the stresses in critical equipment, and power generation, temperatures and pressures in the power plant. Section 3 discusses the control problem in modern NGCCs, the proposed control methodology that accounts for the stresses in thick-walled components, and its mathematical formulation in the form of a quadratic programming problem embedded in an MPC. The results of the tests carried out

using the proposed control methodology are presented in Section 4. Conclusions are summarized in Section 5. Supplementary Material (SM) with a thorough development of the stress and simplified models, and their integration in the optimization problem in the MPC control strategy is provided with this work for the sake of completeness and reproducibility.

2. Power plant description and stress modelling

Several models of different complexity are utilized in this study. A physics-based dynamic model of a NGCC was used to replicate the operation of a modern thermal power plant. As this type of models cannot be implemented in optimization problems due to their complexity and long computational time, simplified models that predict the future state of relevant thermodynamic variables in the NGCC were developed to be included in the optimization problem of the MPC strategy. To predict the thermal and mechanical stresses arising in the high pressure steam drum and in the rotor disk in the first stage of the high pressure steam turbine, physics-based models of these stresses were also developed and included in the optimization problem of the MPC strategy. This section describes these models and provides details about the assumptions considered during their development.

2.1. Natural gas combined cycle dynamic model

Modern natural gas combined cycles are composed of a heavy-duty gas turbine and a triple pressure steam cycle with reheating. In this work, the model also includes steam extraction from the steam turbine and the heat-recovery steam generator (HRSG). The power plant layout is represented in Fig. 1. GT PRO [39] was used to design the NGCC as it provides detailed information of the geometry of the equipment and the materials needed for the dynamic model.

The dynamic full-physics model of the NGCC was developed with the specialized Thermal Power library [40] in the software Dymola [41], based on the Modelica language [42]. As the transient behaviour of thermal power plants is highly dependent on the size of the equipment, dimensions and geometry of the components designed in GT PRO were imported to the dynamic model. Software to software validation at both full and part-load between the Thermoflow and Dymola models was performed. Results were in good agreement. Detailed description of the design, dynamic modelling, and validation of the NGCC dynamic model can be found in the work carried out by Montañés et al. [43].

2.2. Simplified models of the natural gas combined cycle

Model predictive control strategies require the periodic solution of a dynamic optimization problem. The period of time between optimizations, i.e. the sampling time of the MPC, is determined by the dominant dynamics of the system as they indicate when the majority of the transient has occurred. Good control strategies should anticipate the dominant dynamics and act frequently during this period of time. Step responses in the manipulated variables of the MPC with only the drum level controllers switched on showed that the dominant dynamics of the system occur in 250–300 s. Therefore, in order to meet the dynamics of the power plant and have enough time to carry out the dynamic optimization, a sampling time of 30 s was selected. This sampling time prevents the utilization of the dynamic full-physics model in the optimization algorithm and thus simplified models were used instead. System identification [44] was employed to develop a local network of linear ARX models that encompasses the entire power plant operation range [28,45].

System identification refers to the process of constructing dynamic data-based models [44]. Data was obtained from simulations performed in the full-physics dynamic model in Dymola. Closed-loop experiments were carried out because of its superior effectiveness for several applications, specially for control [46,47]. Among the closed-loop
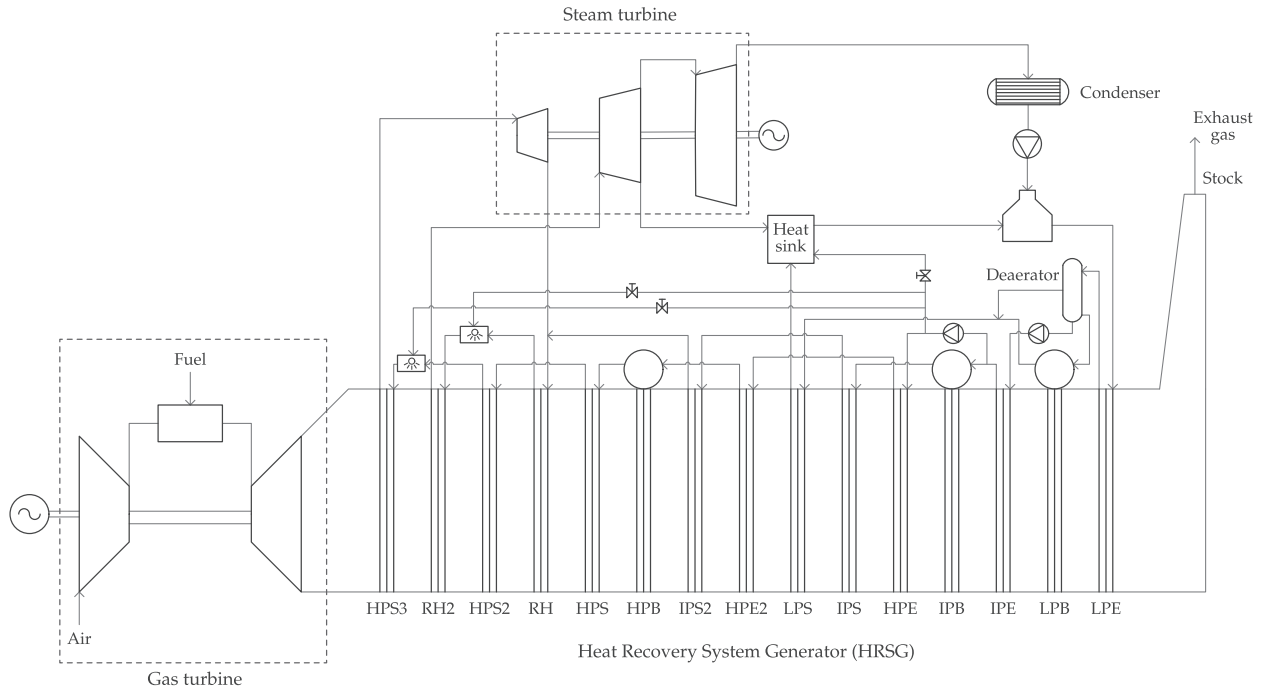
Fig. 1. Process model of the natural gas combined cycle.The nomenclature in the HRSG is as follows. E: Economizer, B: Boiler, S: Superheater, R: Reheater P: Presure, L: Low, I: Intermediate, H: High.

experiment alternatives, a direct approach was followed [44,48]. In this approach, excitation signals are superimposed in the set-points of the controllers of interest, and measurements of the inputs and outputs are collected. All inputs were imposed simultaneously as it leads to better identification of dynamics than doing it individually [49,50]. Pseudo-random binary signals (PRBS) and random Gaussian signals (RGS) were tested as they are persistently exciting and cover properly the input spectrum. Despite that PRBS signals are widely utilized due to their optimum crest factor, RGS proved to lead to better identification.

From this set of data, a model structure was fitted by varying the model parameters. Autoregressive models with exogeneous variable and without noise integration (ARX models) were selected. The general structure of an ARX model is:

$$y(t) + a_1\,y(t-1)+\cdots+a_{n_y}\,y(t-n_y)= \\ b_1\,U(t-1)+\cdots+b_{n_U}\,U(t-n_U) + e(t) \qquad (1)$$

where n_y and n_U represent the number of past outputs and inputs included in the model, and $e(t)$ is a white-noise term that enters the equation as a direct error in the difference equation. If $e(t)$ is considered as the prediction error, the predictor is given in vector form by:

$$\hat{y}(t) = \theta^{\mathrm{T}}\,\varphi(t) = \varphi(t)^{\mathrm{T}}\,\theta \qquad (2)$$

where

$$\theta = \begin{bmatrix} a_1, & a_2,..., & a_{n_y}, & b_1, & ..., & b_{n_U} \end{bmatrix}^T$$

$$\varphi(t) = [-\hat{y}(t-1),...,-\hat{y}(t-n_y),...,U(t-n_U)]^T$$

ARX models are linear and cannot be used to predict the nonlinear behaviour of NGCCs. Consequently, a local model network (LMN) was used to capture and predict the high nonlinearities of the system. This simplified model relies on the development of several local linear models at different operating regimes and their interpolation according to the operating conditions. Nonlinearities can hence be captured by a set linear models with adequate interpolation. Fig. 2 represents the general structure of a local model network with several local models. This approach was firstly proposed by Johansen and Foss [45], and Prasad et al. [28] proved its efficacy for capturing the nonlinear

dynamics of a thermal power plant.

Local ARX models were developed over the operating region of interest of the NGCC. Defining such local regions is an heuristic procedure. The gas turbine load was chosen as the main criterion. Thus, linear models were utilized to predict the nonlinear behaviour around the 100%, 90%, 80%, 70%, and 60% load of the gas turbine. Since the transition among local regions is a smooth process, the local models need to be interpolated accordingly in order to predict the overall plant performance over its global operating region. Neighbouring local models should contribute more to the solution than local models of regimes far from the operating conditions. This is accomplished by
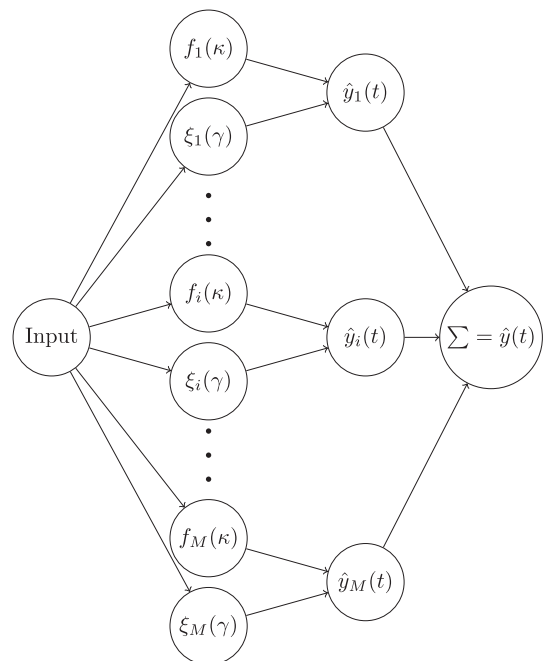

Fig. 2. Structure of a generic local model network.

associating a validity function to each local ARX model and combining all the predicted responses in the final output:

$$\hat{y}(t) = \sum_{k=1}^{M} f_i(\kappa)\, \xi_i(\gamma) \tag{3}$$

where M is the number of local models, $f_i(\kappa)$ is the evaluation of the each ARX model under the conditions defined by κ, ξ is the local validity function associated to each ARX model, and γ is the parameter defining the current operating point, which is the current GT load.

A Gaussian validity function was selected as interpolator of the local models [45]:

$$\xi_i(\gamma) = \frac{exp\left(-\frac{1}{2}\,[(\gamma - c_i)/w_i]^2\right)}{\sum_{k=1}^{M} exp\left(-\frac{1}{2}\,[(\gamma - c_i)/w_i]^2\right)} \tag{4}$$

where c_i and w_i are, respectively, the centres and widths of the local interpolation functions.

As recommended by Johansen and Foss [45] and Prasad et al. [28], the local model and validity function parameters were computed by a nonlinear optimization that aimed at minimizing the global predicting error of the local model network. Local ARX models of second order were considered suitable for predicting the temperature deviation at the outlet of the superheater and reheater. The power plant net power ARX model was selected to be of first order. Linear polynomials were defined to obtain the saturation pressure and temperature in the high pressure drum, and the pressure at the inlet of the steam turbine. Local model and validity function parameters are included in the Supplementary Material (SM).

Validation of the local model network was performed by testing its prediction and interpolation capabilities in the intermediate load ranges, i.e. at 95%, 85%, 75%, and 65% of the GT load. Random Gaussian signals were also utilized to generate the validation data. For the linear polynomials, ramp changes over the NGCC operation range were employed. Table 1 summarizes the validation results based on the R^2 value. Despite the lower values of the model predicting the net power generation of the power plant, the model is capable of predicting the dynamics of the system with high accuracy. These results may be observed in the Supplementary Material (SM) together with all the graphical representation of the validation results.

Because of the linearity of the polynomials and the local models integrating the LMN, this simplified model may be expressed as a linear system of equations. Expanding these simplified models over time, an overall system of equations representing the relation among the responses and manipulated variables in a finite time horizon is achieved. Therefore, this system can be written as:

$$A_{\mathrm{LMN}} X_{\mathrm{LMN}} = b_{\mathrm{LMN}} \tag{5}$$

where X_{LMN} is the vector containing the different predicted responses, y, and manipulated variables, U, in a time horizon. Matrix A_{LMN} and vector b_{LMN} are defined in the Supplementary Material (SM).

2.3. Thermal and mechanical stress modelling

Thick-walled components are the most sensitive equipment in NGCCs as large temperature differences that lead to thermal stresses arise in the wall. In addition, mechanical stresses are present as these components are exposed to the highest pressures of the power plant and may be subjected to rotation. Adequate control of combined cycles must hence ensure the operating conditions do not damage this critical equipment. The high pressure drum and the high pressure steam turbine rotor disk were the components considered in this work. Because of their geometry, plane strain was assumed in the steam drum and plane stress was considered in the rotor.

The temperature profile along the wall is required to compute the thermal stresses. Temperature was assumed to vary in radial direction

and thus its distribution is obtained from the one-dimensional heat equation in radial direction:

$$\frac{1}{r}\frac{\partial}{\partial r}\left(r\frac{\partial T}{\partial r}\right) = \frac{1}{\alpha}\frac{\partial T}{\partial t} \tag{6}$$

An implicit Crank-Nicolson discretization scheme was utilized to compute the temperature distribution along the wall. Both drum and rotor encounter different fluids and thermodynamic states in their inner and outer surfaces. The high pressure drum is on contact with saturated water and steam on the inner surface and with air in the outer, whereas the high pressure turbine rotor is in contact with superheated steam on the outer surface and the shaft at an unknown state on the inner wall. Therefore, different boundary conditions must be imposed. The implementation of the different boundary conditions is detailed in the Supplementary Material (SM).

Thermal and mechanical stresses were modelled together following a common approach for both plane stress and plane strain. Given the constitutive equations that relate the stress with the strain and combining them with the strain-displacement relations, the stress in each direction can be expressed in terms of the displacement and the temperature in radial direction [51]. Inserting these equations into the radial equilibrium equation, an ordinary differential equation relating the displacement with the temperature gradient and the centrifugal force due to rotation is obtained [51]. Pressure enters in these equations as boundary conditions in the radial stress equation. The systems of equations for the cases of plane strain and plane stress are defined in Eqs. (2) and (3), respectively.

$$\frac{d^2u}{dr^2} + \frac{1}{r}\frac{du}{dr} - \frac{u}{r^2} = \frac{(1+\upsilon)}{(1-\upsilon)}\alpha^*\frac{dT}{dr} - \frac{(1-2\upsilon)(1+\upsilon)}{(1-\upsilon)}\rho\omega^2 r \tag{7a}$$

$$\sigma_r = \frac{E\upsilon}{(1-2\upsilon)(1+\upsilon)}\left[\frac{1-\upsilon}{\upsilon}\frac{du}{dr} + \frac{u}{r}\right] - \frac{E\alpha^*}{1-2\upsilon}T \tag{7b}$$

$$\sigma_\theta = \frac{E\upsilon}{(1-2\upsilon)(1+\upsilon)}\left[\frac{du}{dr} + \frac{1-\upsilon}{\upsilon}\frac{u}{r}\right] - \frac{E\alpha^*}{1-2\upsilon}T \tag{7c}$$

$$\sigma_z = \frac{E\upsilon}{(1-2\upsilon)(1+\upsilon)}\left[\frac{du}{dr} + \frac{u}{r}\right] - \frac{E\alpha^*}{1-2\upsilon}T \tag{7d}$$

$$\frac{d^2u}{dr^2} + \frac{1}{r}\frac{du}{dr} - \frac{u}{r^2} = (1+\upsilon)\alpha^*\frac{dT}{dr} - \frac{1-\upsilon^2}{E}\rho\omega^2 r \tag{8a}$$

$$\sigma_r = \frac{E}{1-\upsilon^2}\left[\frac{du}{dr} + \upsilon\frac{u}{r} - (1+\upsilon)\alpha^*T\right] \tag{8b}$$

$$\sigma_\theta = \frac{E}{1-\upsilon^2}\left[\upsilon\frac{du}{dr} + \frac{u}{r} - (1+\upsilon)\alpha^*T\right] \tag{8c}$$

The stress components in the different directions are combined in an scalar measure of the overall equivalent, or effective, stress. This

Table 1
Validation R^2 results for the local network of ARX models and linear polynomials.

Variable	Symbol	GT Load				
		95%	85%	75%	65%	Ramp
Net Power	y_1	61.77%	76.11%	74.97%	73.97%	–
Superheated Steam Temperature	y_2	95.51%	98.40%	99.03%	99.14%	–
Reheated Steam Temperature	y_3	93.18%	94.65%	90.37%	92.49%	–
Turbine's Steam Inlet Pressure	y_4	–	–	–	–	86.16%
Drum's Saturation Temperature	y_5	–	–	–	–	85.22%
Drum's Saturation Pressure	y_6	–	–	–	–	86.62%

parameter can be implemented as a constraint in the optimization problem included in the MPC strategy. The von Mises equivalent stress defined in Eq. (9) is used as this measure.

$$\sigma_{\text{eff}}^2 = \sigma_r^2 + \sigma_\theta^2 + \sigma_z^2 - (\sigma_r \sigma_\theta + \sigma_\theta \sigma_z + \sigma_z \sigma_r) \qquad (9)$$

Since the von Mises equivalent stress is a nonlinear equation and linear MPC is the proposed control strategy, a linearisation of the von Mises equivalent stress is used to integrate the equivalent stress in the linear optimization algorithm:

$$\sigma_{\text{eql}}^2 = \sigma_{\text{eql},0}^2 + \nabla \sigma_{\text{eql},0}^2 \Delta \sigma + \mathcal{O}(\Delta x^2) \qquad (10)$$

These stress equations are discretized with central finite differences and combined with the temperature distribution expressions in a common system of equations that allows to compute simultaneously the temperature, the displacement, each of the stress components and the linearised von Mises effective stress. Combining these system of equations over time, the evolution of these variables in both space and time can be obtained from a larger system of equations:

$$A_{\text{drum}|\text{rotor}} X_{\text{drum}|\text{rotor}} = B_{\text{drum}|\text{rotor}} \qquad (11)$$

where $X_{\text{drum}|\text{rotor}}$ is a vector containing the temperature difference from the design point, the displacement and the stresses in the wall discretizations over time. $A_{\text{drum}|\text{rotor}}$ and $B_{\text{drum}|\text{rotor}}$ are defined for both components in the Supplementary Material (SM).

The temperature and stress models where implemented in MATLAB [52] and validated in the specialized software ANSYS [53]. Structural steel was assumed as the material to ensure well-known physical properties in both models. A time discretization of 1 s was selected, whereas 50 and 800 spatial discretizations were chosen for the rotor and drum, respectively. Heating and cooling of both components was implemented by steam temperature ramp changes in the boundary conditions. A summary of the boundary conditions imposed during the validation is presented in Table 2. Figs. 3 and 4 represent, respectively, the drum and rotor validation results at six different radii.

3. Control methodology for optimal operation accounting for stresses

Control of thermal power plants matches generated power to the power demand from the electrical grid, and modifies adequately the temperatures, pressures and mass flows to ensure a safe, stable and efficient operation. This section presents the control problem encountered in modern NGCCs, describes the proposed methodology to optimally control the power plant whilst monitoring the stresses in critical equipment, and details its implementation as a quadratic optimization program embedded in an MPC.

3.1. Control problem

Natural gas combined cycles are integrated by two thermodynamic cycles characterized by different dynamics. Gas turbines are fast components that can adapt their operation within seconds. In contrast, steam bottoming cycles are slow units limited by the large heat capacitance of the heat-recovery steam generator, as it induces delays of 10–20 min with respect to the gas turbine operation [54,55]. Therefore,

power control in modern NGCCs is achieved by adjusting the gas turbine load. The steam cycle follows the gas turbine operation acting as a passive element that generates power with the steam available in the HRSG.

The operation of the gas turbine is determined by the performance map of its components. Automatic control is normally incorporated in these units to ensure high turbine inlet and exhaust temperatures at nominal and part-loads down to 40% [54]. This control is achieved by adapting the variable guide vanes (VGV) of the compressor, which modify the air flow rate. As gas turbines have almost negligible dynamics compared with those of the steam cycle and their operating conditions may be defined by their load, a quasi-static model is utilized in this work to represent the gas turbine. Exhaust gas mass flow and temperature are hence determined by the load control assuming immediate adjustment of fuel mass flow and VGV position. These are the boundary conditions imposed on the steam cycle [13].

The operation of the steam cycle is based on sliding pressure. In this operation strategy, the admission valves of the steam turbine are close to fully open, allowing the pressure upstream of the steam turbine to vary freely. This keeps the volume flow close to constant in the steam turbine at part load, leading to evenly distributed pressure ratios that reduce the temperature gradients within the turbine and to high isentropic efficiency at different operating conditions [56]. Sliding pressure operation may be applied until 50% load, after which throttling control is required [54]. Therefore, for the power generation changes considered in this work, steam pressure control is not necessary. Control of the steam bottoming cycle is hence reduced to inventory control of the steam drums and condenser, pressure control of the low pressure drum and the deaerator, and limiting the superheated and reheated steam temperature. Furthermore, this work proposes the control of the stresses developing in thick-walled components, as excessively fast load changes may lead to stresses that can damage this equipment.

3.2. Control methodology

A regulatory control layer is utilized in the control strategy of the natural gas combined cycle to stabilize its operation. This includes the level control of the intermediate and high pressure drums and the condenser, and the pressure control of the deaerator and the low pressure drum. Three-element controllers are normally utilized to control the drum level [54]. In this type of controller, the drum level, the feedwater flow and the live-steam flow are processed with a PID cascade structure that acts on the feedwater valves [43]. The low pressure of the cycle is controlled with a PI controller that measures the pressure in the deaerator and acts on the low pressure valve. A detailed diagram of this control structure can be found in the work by Montañés et al. [43].

Model predictive control is utilized to control the power generation of the NGCC, the superheated and reheated steam temperatures, and the maximum stresses arising in the considered components. Power generation is controlled by modifying the gas turbine load, whilst two attemperator valves are used to limit the superheated and reheated steam temperatures. Stress control is achieved by limiting the ramp changes of the gas turbine. This leads to slower changes in the steam cycle, which result in smaller temperature gradients and slower

Table 2
Validation boundary conditions.

| Component	Thermal Boundary Conditions				Mechanical Boundary Conditions		Rotation
	T_{initial}	Ramp	h_{i}	h_{o}	r_{i}	r_{o}	
Drum	340 [°C]	± 20	20000 [W/m^{2}K]	0.065 [W/m^2°C]	p = 150 [bar]	p = 1 [bar]	–
Rotor	590 [°C]	± 10	–	20000 [W/m^2°C]	u = 0 [m]	p = 140 [bar]	3000 [rpm]

pressure variations in the high pressure drum and rotor. Therefore, the effective stress in thick-walled components is reduced by limiting the maximum load ramps of the gas turbine.

Linear quadratic control, i.e. an MPC strategy based on a quadratic programming optimization problem, was selected because of its fast computational time and convexity [57]. This type of optimization problems guarantees that global minima are found if the weight matrices are defined adequately [57]. The simplified models predicting the performance and key thermodynamic variables in the NGCC are combined with the physics-based stress models in a linear system of equations that enters the optimization problem as linear equality constraints. This methodology ensures that optimal control actions that respect the stress constraints in specific equipment and the behaviour of the NGCC are thus computed.

Since the gas turbine and steam cycle have different dynamics, an extra linear MPC that only regulates the power of the gas turbine was included. The sampling time of this control is 5 s as the gas turbine dynamics are almost negligible. This control aims at complementing the global MPC with more frequent power control and at narrowing the gap between the demand and the production. With this overall control strategy, the global MPC defines the control actions that stabilize the NGCC every 30 s while the GT MPC adjusts the gas turbine load every 5 s. If the difference between the current stress in the critical components and the maximum allowable effective stress is less than 15%, it is considered that the steam cycle's dynamics dominate the power plant operation and hence the global MPC sets the control actions without inputs from the GT MPC. This approach ensures that when there is not enough margin between the current stress in the drum and rotor and their limit, the global MPC accounts for the stresses that may arise, whereas when the difference is large the GT MPC acts more frequently to meet the power demand.

A schematic representation of the control strategy of the NGCC is presented in Fig. 5. The physics-based NGCC dynamic model represents the operation of an actual power plant with a regulatory control layer already implemented. Measurements of key parameters, e.g. temperatures, pressures and mass flow rates, are fed into both global and GT MPC, where dynamic optimizations are carried out every 30 and 5 s. The solution of these optimization problems are the optimal control
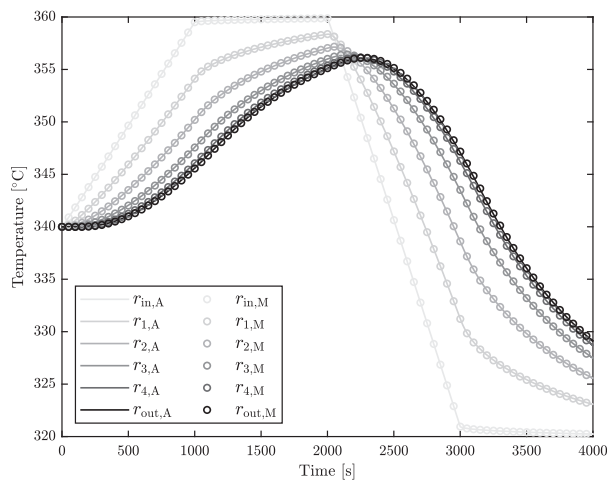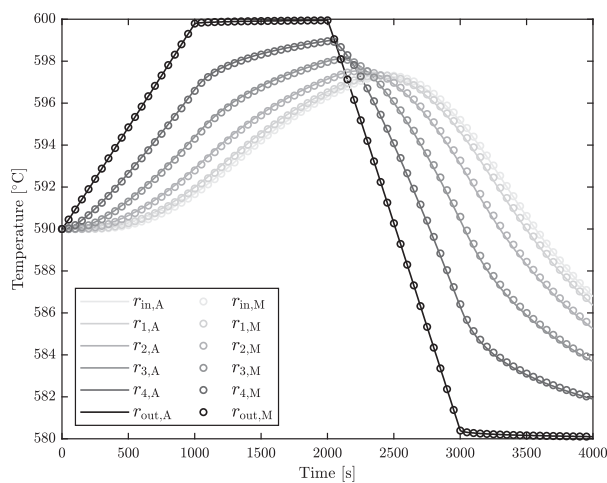

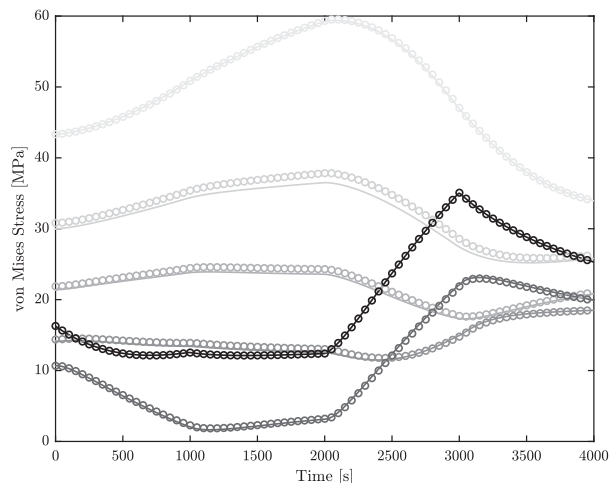(a) Temperature along six equidistant radii. A refers to ANSYS and M to MATLAB.
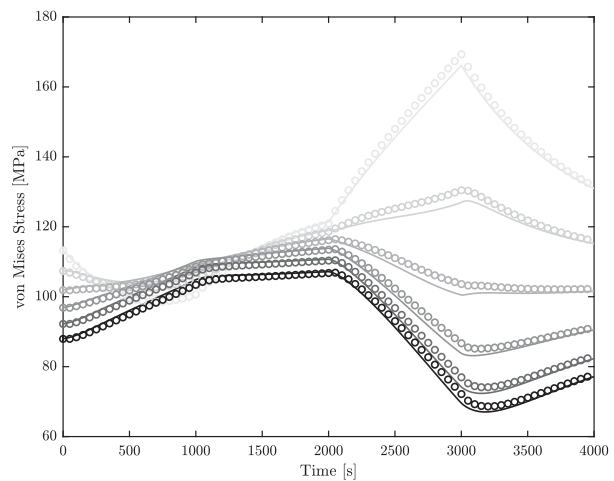
(b) von Mises equivalent stress along six equidistant radii.

Fig. 3. Validation results for the drum model.

(a) Temperature along six equidistant radii. A refers to ANSYS and M to MATLAB.

(b) von Mises equivalent stress along six equidistant radii.
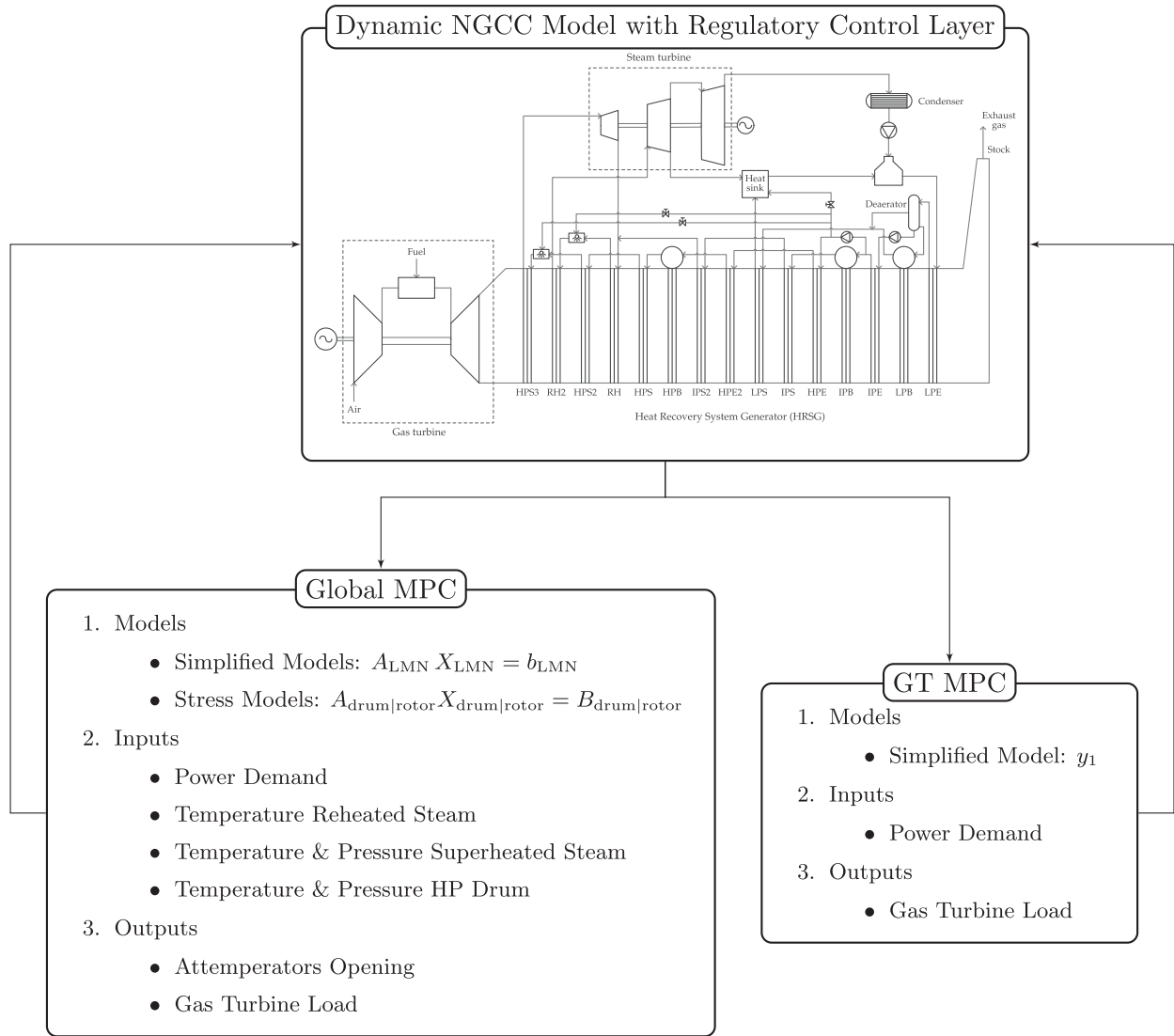
Fig. 4. Validation results for the rotor model.

Fig. 5. Structure of the proposed control methodology accounting for stresses in critical components.

actions that must be imposed in the power plant. The novelty and strength of the proposed control methodology lies in the global MPC, as optimal control actions are computed simultaneously with the stresses arising in critical equipment in an optimization framework. This ensures that the implementation of the computed control actions will not lead to excessive stresses in the equipment of the actual NGCC.

3.3. Model predictive control formulation

The optimal quadratic programming (QP) control problem represented by both global and GT linear MPCs is formulated as:

$$\min_{z \in \mathbb{R}^n} f(z) = \frac{1}{2} z^\mathrm{T} Q z + d z \tag{12a}$$

subject to

$$A_\mathrm{eq} \, z = B_\mathrm{eq} \tag{12b}$$

$$A_\mathrm{ineq} \, z \leqslant B_\mathrm{ineq} \tag{12c}$$

$$z^\mathrm{low} \leqslant z \leqslant z^\mathrm{high} \tag{12d}$$

with

$$Q \succcurlyeq 0 \tag{12e}$$

In the global MPC, vector z contains X_LMN, X_drum and X_rotor. It represents the optimal sequence of responses, control inputs, and temperature, displacement and stresses in both drum and rotor for several space and time discretizations calculated over a time horizon N. These variables are the dynamic optimization variables and are limited by lower and upper bounds (Eq. (12d)), ensuring that the maximum allowable stress in both drum and rotor is never exceeded. This optimization problem is subject to linear constrains (Eq. (12b)) that ensure the simplified models (Eq. (5)) and the drum and rotor stress models (Eq. (11)) are satisfied. In addition, linear inequality constraints (Eq. (12c)) are included in order to limit the load ramps in the gas turbine. The degrees of freedom included in vector z are modified throughout the optimization to minimize the objective function $f(z)$ in Eq. (12a). The objective function considered in this work aims at minimizing the difference between the power generation and demand, and the deviation of both superheated and reheated steam temperatures from their nominal value. The description of these matrices and vectors is included in the Supplementary Material (SM).

In the GT MPC, vector z includes the optimal sequence of net power generation and gas turbine loads throughout the time horizon. Therefore, the LMN for these two variables is the only equality constraint, and the maximum gas turbine load gradient is the only inequality constraint. Lower and upper bounds are also included for both
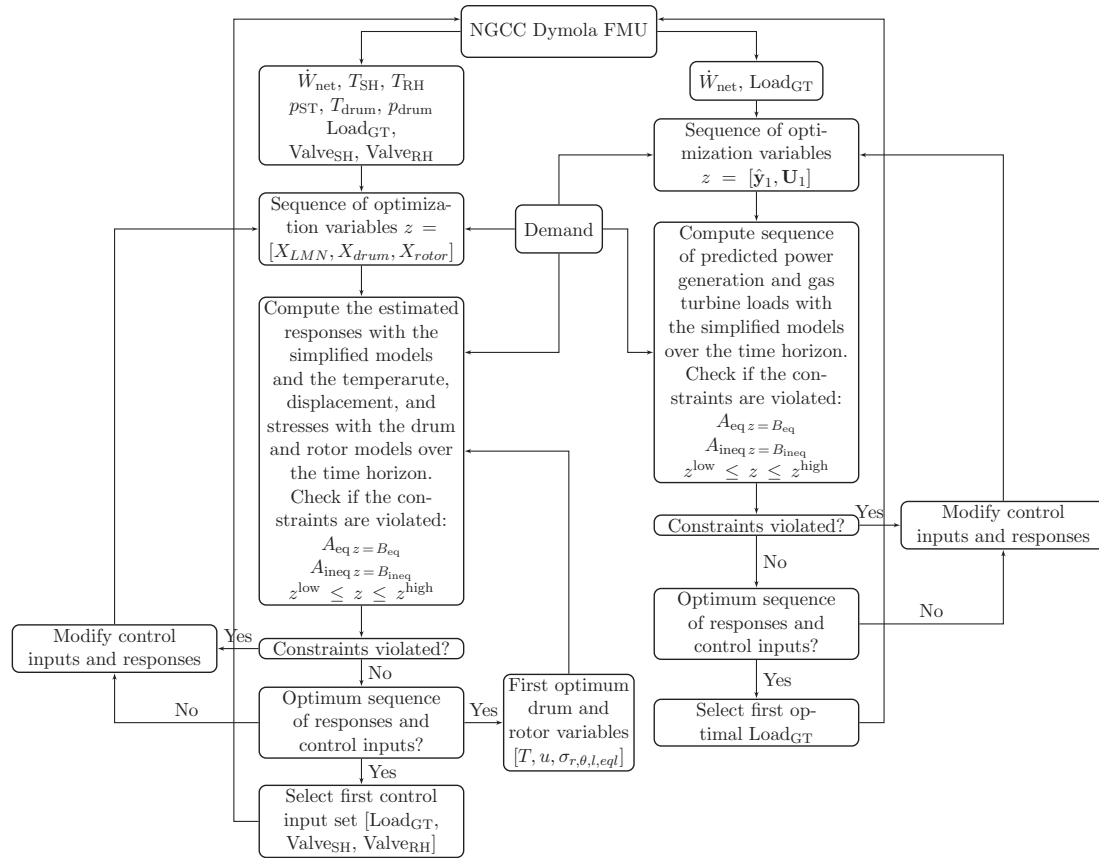
Fig. 6. Logic diagram of the MPC control strategy.

Table 3
Materials' physical and mechanical properties.

Component	Material	ρ [kg/m³]	C_m [J/kg K]	k_m [W/m K]	α^* [m²/s]	α [1/K]	E [MPa]	υ [–]	h_o [W/m² K]	h_i [W/m² K]	Yield stress [MPa]
Drum	SA-515 Grade 70	7850	434	47	1.3796e-05	1.36e-5	178000	0.3	5000	0.065	190
Rotor	X18CrMnMoNbVN12	7700	460	29	8.1875e-06	1.25e-5	127000	0.292	4000	–	69

variables. The detailed description of this GT MPC is also included in the Supplementary Material (SM).

A diagram representing the logic of the MPC-based control methodology for the NGCC is illustrated in Fig. 6. The full-physics dynamic

model developed in Dymola and the optimization algorithm in the MPC developed in MATLAB were merged in Simulink through a Functional Mock-up Unit (FMU). This FMU containing the detailed dynamic model of the NGCC with the regulatory control layer represents an actual
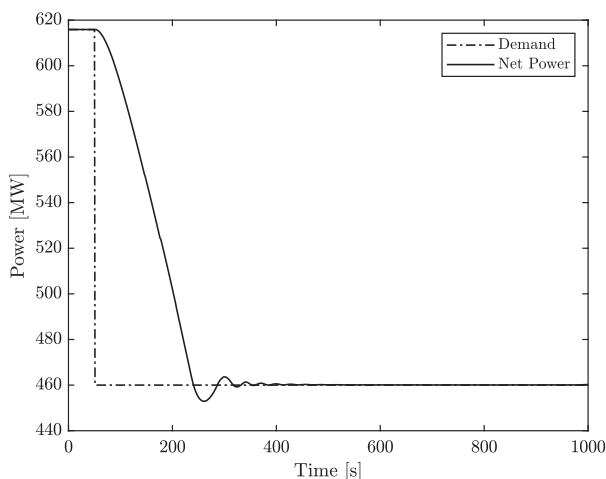
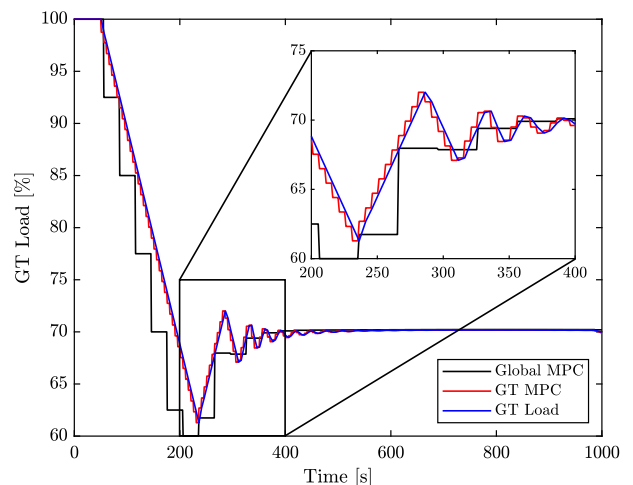**Fig. 7.** Net power generation of the natural gas combined cycle.

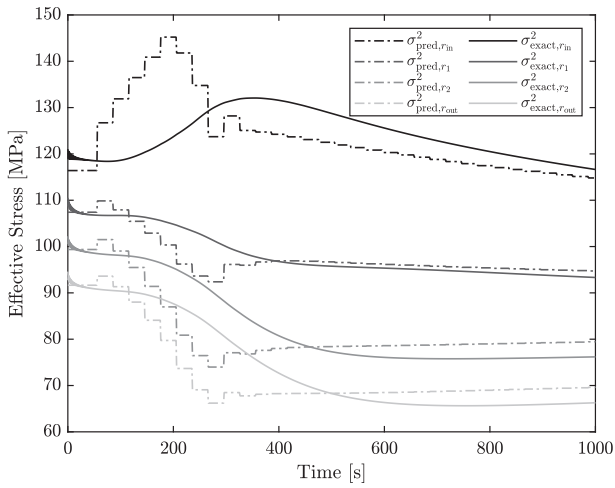**Fig. 8.** Load profile of the gas turbine with MPC optimization steps.

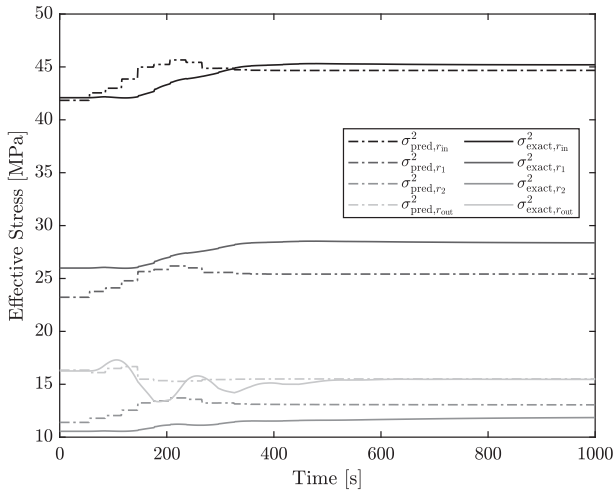Fig. 9. Estimated and exact equivalent stress in the drum at different radii.

Fig. 11. Control of the superheat steam temperature.

Fig. 10. Estimated and exact equivalent stress in the rotor at different radii.
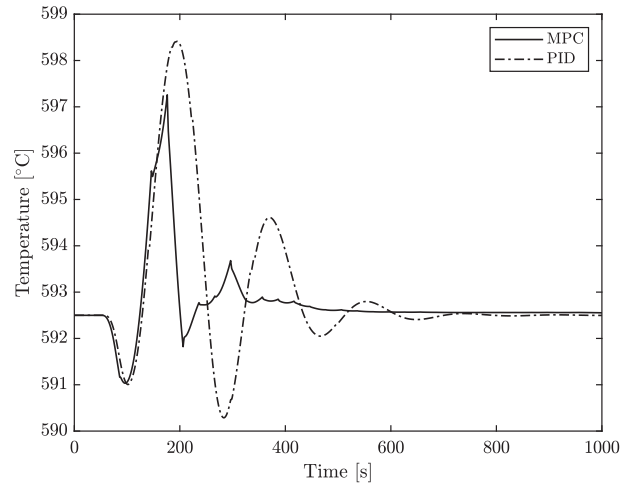
Fig. 12. Control of the reheat steam temperature.

NGCC, and provides the measurements of key parameters that are required in both MPCs to compute the optimal control actions.

4. Results and discussion

Load step change is a suitable scenario to test the control capabilities of the methodology proposed in this work. A step change in the power demand of 165 MW drives the transient operation of the natural gas combined cycle. The main goal is to minimize the difference between the power demand and generation as fast as possible while satisfying the constraints of the system. Two cases are studied in order to present the control capabilities of the proposed methodology. First, the performance of the NGCC during the load ramp is analysed under reasonable stress limitations that can be expected in current modern power plants. Subsequently, the same dynamic behaviour is studied under tight constraints on the allowable stress of the steam drum, as it represents possible scenarios as start-ups. Table 3 includes the materials considered in this work for the drum and rotor as well as their physical and mechanical properties. The yield stress of the drum utilized in the second analysis is 130 MPa instead of 190 MPa to guarantee that the constraint is active.

The weights in the matrix and vector of the objective function in the global MPC are $\lambda_{y_1} = 1$, $\lambda_{y_2} = \lambda_{y_3} = 10$, and $\lambda_{U_1} = \lambda_{U_2} = \lambda_{U_3} = 2$ (see Supplementary Material (SM)). In the GT MPC, $\lambda_{y_1} = 1$ and $\lambda_{U_1} = 0.1$. A time horizon of 30 sampling times was considered to guarantee that the
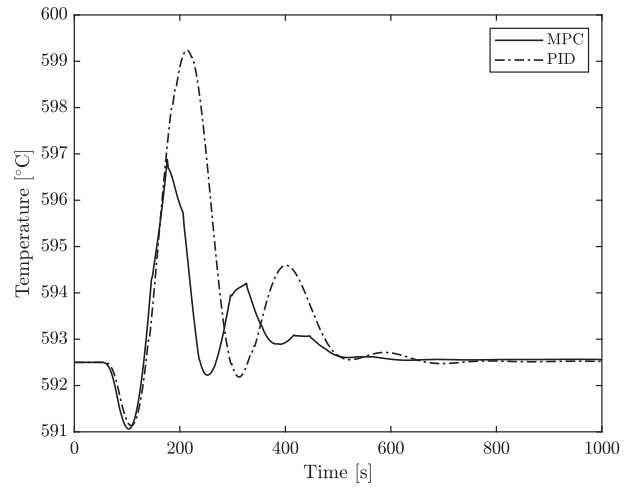
system dynamics are captured, 200 and 50 spatial discretizations were used in the drum and rotor walls respectively, and 3 time discretizations per sampling time were utilized.

4.1. Optimal dynamic operation with realistic constraints

In this first case the transient performance of the NGCC is studied by imposing constraints that may be expected in modern power plants. This includes gas turbine load ramping rates up to 15% per minute, and complex alloys for the rotor material capable of withstanding the high temperature and pressure at the inlet of the steam turbine [58].

With these constraints imposed, the NGCC is able to meet the power demand in 300 s (see Fig. 7). Since this time is half the stabilization time of the steam cycle, it is clear that the gas turbine compensated the slow response of the HRSG. This behaviour is represented in Fig. 8. The gas turbine load is under-shot in order to compensate the slow transient of the steam cycle and meet the power demand faster. As the steam cycle reaches steady-state at part-load, the gas turbine increases progressively its load to keep the power generation constant. The GT stops fluctuating after 600 s, which coincides with the stabilization time of the steam cycle.

From a dynamic optimization perspective, the load of the gas turbine is always dictated by the GT MPC, which finds a different and smoother optimal trajectory than the global MPC as it is evaluated more frequently. This is possible since the difference between the equivalent
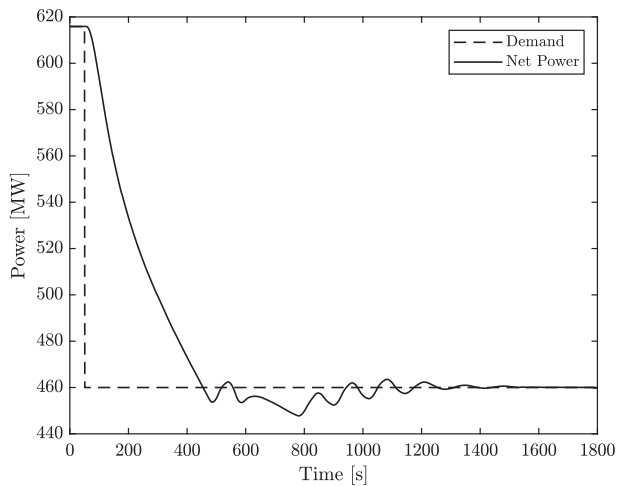
Fig. 13. Net power generation of the natural gas combined cycle.

Fig. 14. Load profile of the gas turbine with MPC optimization steps.

stress in both drum and rotor and the maximum allowable stress is always bigger than 15%. Figs. 9 and 10 show the stresses predicted by the global MPC at each sampling time during the transient operation of the NGCC.

The stress in both components was calculated with the exact profile of temperatures and pressures from the dynamic high-fidelity model and compared with the linearized equivalent stresses predicted during the dynamic optimizations (see Figs. 9 and 10). Despite the predicted stress overestimated slightly the equivalent stress in both components, both in time and magnitude, it predicts adequately their tendency and the largest value, ensuring that the components do not exceed the maximum allowable limit. This discrepancy may be generated by the utilization of simplified models and the lack of detailed wall temperatures from the dynamic high-fidelity model. The simplified models might over-predict the rate of change of the temperature and pressure in both components, leading to faster dynamics than those encountered in the detailed model. However, the the lack of detailed wall temperature in the dynamic high-fidelity model may influence more the difference between the predicted and exact stresses, as it prevents the utilization of actual wall temperatures and forces the estimation of the initial conditions along the wall at each optimization. Having detailed data of the wall temperature every sampling time would smear out the fluctuations of the stress predictions.

Superheat and reheat steam temperature profiles with PID controllers in the attemperators were also calculated by imposing the gas turbine load profile in the detailed dynamic model. The results are represented in Figs. 11 and 12. Albeit being more aggressive, MPC outperforms the PID temperature controllers as it is able to stabilize the superheated and reheated steam temperatures faster and with smaller deviations from their set-point.

During this transient response the inequality constraint limiting the maximum gas turbine load gradient is always active for both MPC controllers. Therefore, it is the gas turbine and not the stresses in thick-walled components the main limitation for faster and more flexible operation of natural gas combined-cycles during load changes. On the contrary, during the start-up of the power plant, it is expected that the stresses in these components are the limiting factor for faster operation. Consequently, in order to prove that this control methodology is suitable also for start-up of natural gas combined cycles, the same scenario is studied but ensuring that the maximum allowable stress is reached in the steam drum. This was done by reducing the yield stress limit to 130 MPa.

4.2. Optimal dynamic operation with tight stress constraints

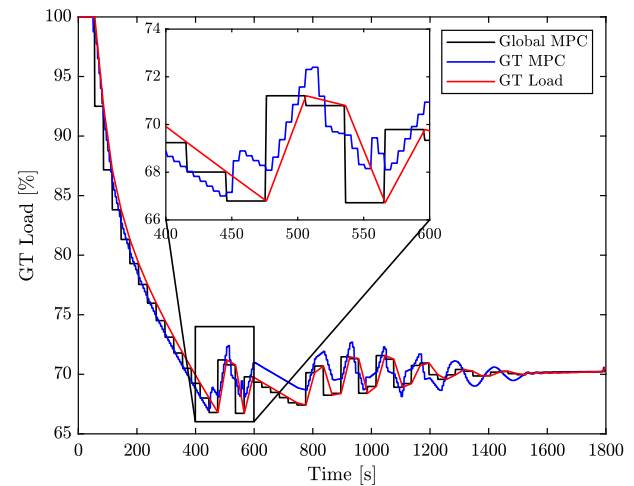This case aims at showing the capabilities of the methodology

proposed in this work to control the power generation of the NGCC under tight constraints imposed on the material of the equipment. Fig. 13 shows the net power generation of the NGCC for these tight constraints. As expected, the power plant requires more time to meet the power demand since the stress limitation in the drum inhibits large changes in the gas turbine load. Thus, and since the stabilization time is longer than the 600 s required by the steam cycle, the stress in the high pressure drum is the limiting factor during the transient operation of the NGCC.

The slow transient response of the gas turbine is represented in Fig. 14. In contrast with the previous case, the gas turbine load is dictated by the global MPC, which leads in this case to a smoother gas turbine control. As the margin between the maximum allowable stress and the stress predicted by the global MPC is small, the GT MPC does not influence the power plant operation.

From Fig. 15 can be observed that the constraint on the maximum effective stress in the drum is active for a period of time during the transient. This indicates that the MPC control strategy is able to adequately predict the stress in the steam drum and obtain an optimal control sequence that does not exceed the material allowable limits. The comparison of the exact and the predicted effective stress in Figs. 15 and 16 shows better agreement than in the previous case. This is a result of the slower gas turbine load changes, leading to more uniform conditions in the wall, which, in turn, make the predictions of the initial conditions in the drum more accurate. This fact points out the necessity of incorporating models to calculate the temperature profile along the components wall in the dynamic high-fidelity models. As occurred in the previous case, the abrupt step occurring in the effective drum stress at the first instant after the step change in the power demand may be originated by the simplified models, which over-estimate the dynamic response of the pressure and temperature on the inner surface of the drum.

5. Conclusions

This work proposes a control methodology based on linear MPC with stress control. In the proposed methodology, the effective stress in the high pressure drum and steam turbine inlet rotor are computed and predicted together with relevant thermodynamic variables in specific locations of the steam cycle in an optimization framework. Constraints on the effective stress arising in critical equipment can be imposed with this approach, which allows to compute optimal control actions that do not exceed these material limitations.

Temperature and stress models for the wall of the drum and rotor were developed and validated with finite element method software, whilst simplified ARX and linear polynomial models were created to
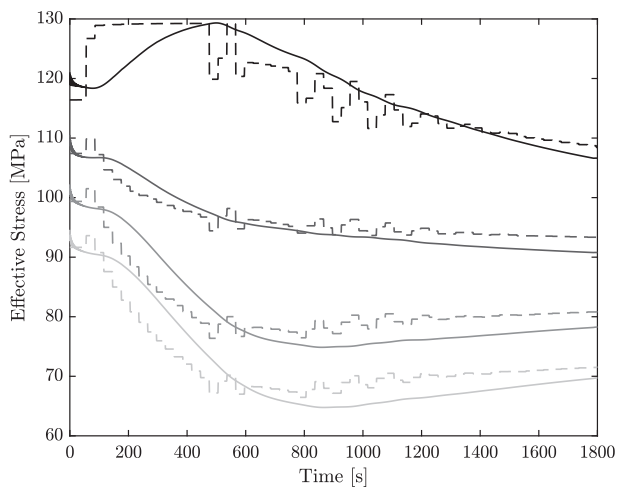
Fig. 15. Estimated and exact equivalent stress in the drum at different radii.

Fig. 16. Estimated and exact equivalent stress in the rotor at different radii.

predict key thermodynamic variables in the steam cycle such as temperatures and pressures during the optimization. The stress and simplified power plant models were embedded as linear equality constraints in the quadratic optimization algorithm within the MPC strategy, which computes the optimal set of control actions and implements them in the thermal power plant every sampling time.

Two cases that simulated load step changes of the NGCC were presented. The first case imposed constraints equivalent to those encountered in modern combined cycles, whereas the second case drastically reduced the maximum allowable stress in the steam drum. The results showed the NGCC is able to reduce the load by 165 MW in 300 s by under-shooting the GT load to compensate the slow transient behaviour of the steam cycle. In this case, the GT MPC defined the load profile of the gas turbine because of the broad margin between the effective and maximum allowable stress in the critical equipment. When the stress limitations were tighter as in the second case, the global MPC defined the gas turbine load profile as the maximum allowable stress limited the ramping capabilities of the NGCC. These results demonstrate that the maximum gas turbine load gradient, and not the stresses in critical components, is the main limitation of flexible natural gas combined cycles during load changes. Therefore, improvements towards enhanced flexibility of this type of thermal power plants requires gas turbines capable of ramping up and down faster.

A comparison in these two cases between the exact and predicted linearised equivalent stress in both drum and rotor showed a good agreement of the results. Despite the simplified models may lead to over-prediction in the initial stress dynamics, it is considered that the discrepancy between predicted and exact effective stresses was originated by the lack of detailed wall temperatures from the dynamic high-fidelity model and thus the need of estimating these initial optimization conditions. Nevertheless, the exact stress never exceeded the stress predicted by the MPC. Thus, the proposed methodology proved to be an effective control strategy suitable to incorporate technical constraints as stress limits in different components and with a faster response and less overshooting in process variables than traditional feedback control strategies.

This control methodology based on MPC with stress control can be extended to other components such as pipes, headers, downcomers, casings or combustors, if stress models for these components are available. The main limitation is the computational time, as more models add more optimization variables to the dynamic optimization problem, which has to be solved within the sampling time spam. Furthermore, the methodology can only handle linear or linearised constraints and nonlinear stress models cannot be included. The methodology proposed in this work could be extended to nonlinear MPC. This is a research gap that must be considered for complicated
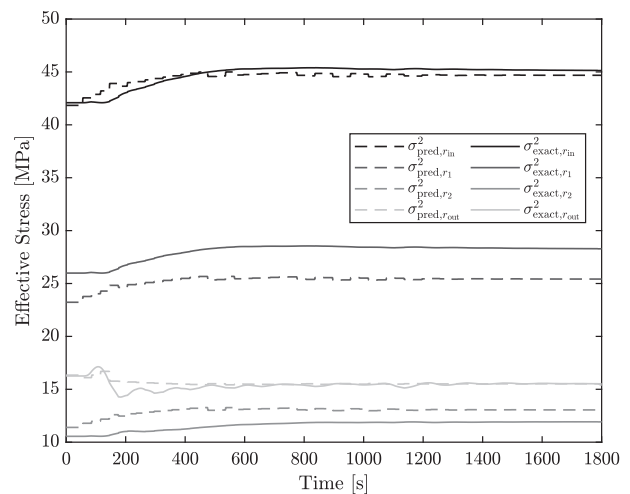
geometries that lead to nonlinear stress models.

The application of this methodology to start-ups and shut-downs of thermal power plants to obtain optimal operating sequences is a promising future research step, as stress limitations dominate the time required in this type of operation. Moreover, the flexibility of this methodology allows to tune the objective function to explore different control actions, include online model estimation to account for changes in the power plant such as fouling, and easily include Kalman filters or additional variables that may be needed during the start-up as, for instance, bypass valves and steam mass flow and temperature prediction models in different location of the steam cycle. This methodology could also be combined with fatigue analysis in an economic MPC, where the objective may be to find a trade-off between the damage in specific equipment and the economic revenue from gas turbine ramps or start-ups and shut-downs. Scheduling will be a relevant issue in future power markets, and combining stress and fatigue analyses with power plant control and damage studies can lead to economic benefits.

Declaration of Competing Interest

The authors declare that they have no known competing financial interests or personal relationships that could have appeared to influence the work reported in this paper.

Acknowledgements

Appendix A. Supplementary material

Supplementary data associated with this article can be found, in the online version, at https://doi.org/10.1016/j.applthermaleng.2019. 114858.

References

[1] IPCC, Summary for Policymakers, in: Global warming of 1.5C. An IPCC Special Report on the impacts of global warming of 1.5C above pre-industrial levels and related global greenhouse gas emission pathways, in the context of strengthening the global response to the threat of climate change, sustainable development, and efforts to eradicate poverty, [V. Masson-Delmotte, P. Zhai, H.O. Pörtner, D. Roberts, J. Skea, P.R. Shukla, A. Pirani, W. Moufouma-Okia, C.Péan, R. Pidcock, S. Connors,

J.B.R. Matthews, Y. Chen, X. Zhou, M.I. Gomis, E. Lonnoy, T. Maycock, M. Tignor, T. Waterfield (eds.)]. World Meteorological Organization, Geneva, Switzerland, 2018.

[2] IPCC, Climate Change 2014: Synthesis Report, Contribution of Working Groups I, II and III to the Fifth Assessment Report of the Intergovernmental Panel on Climate Change [Core Writing Team, R.K. Pachauri and L.A. Meyer (eds.)], IPCC, Geneva, Switzerland, 2014.

[3] International Energy Agency – IEA, World Energy Outlook 2018: Executive Summary, 2018. https://webstore.iea.org/download/summary/190?fileName= English-WEO-2018-ES.pdf.

[4] European Commission, Energy Roadmap 2050, 2011. https://eur-lex.europa.eu/ LexUriServ/LexUriServ.do?uri=COM:2011:0885:FIN:EN:PD.

[5] J. Bertsch, C. Growitsch, S. Lorenczik, S. Nagl, Flexibility in Europe's power sector: an additional requirement or an automatic complement? Energy Econ. 53 (2016) 118–131.

[6] M. Huber, D. Dimkova, T. Hamacher, Integration of wind and solar power in Europe: assessment of flexibility requirements, Energy 69 (2014) 236–246.

[7] H. Kondziella, T. Bruckner, Flexibility requirements of renewable energy based electricity systems–a review of research results and methodologies, Renew. Sustain. Energy Rev. 53 (2016) 10–22.

[8] R.M. Montañés, M. Korpås, L.O. Nord, S. Jaehnert, Identifying operational requirements for flexible CCS power plant in future energy systems, Energy Procedia 86 (2016) 22–31.

[9] J. Oswald, M. Raine, H. Ashraf-Ball, Will British weather provide reliable electricity? Energy Policy 36 (8) (2008) 3212–3225.

[10] International Energy Agency – IEA, Technology Roadmap, Energy storage, 2014. https://www.iea.org/publications/freepublications/publication/ TechnologyRoadmapEnergystorage.pdf.

[11] P. Eser, N. Chokani, R. Abhari, Operational and financial performance of fossil fuel power plants within a high renewable energy mix, J. Glob. Power Propul. Soc. 1 (2017) 16–27.

[12] M.A. González-Salazar, T. Kirsten, L. Prchlik, Review of the operational flexibility and emissions of gas-and coal-fired power plants in a future with growing renewables, Renew. Sustain. Energy Rev. 82 (2017) 1497–1513.

[13] F. Alobaid, N. Mertens, R. Starkloff, T. Lanz, C. Heinze, B. Epple, Progress in dynamic simulation of thermal power plants, Prog. Energy Combust. Sci. 59 (2017) 79–162.

[14] L. Riboldi, L.O. Nord, Optimal design of flexible power cycles through Kriging-based Surrogate models, in: ASME Turbo Expo 2018: Turbomachinery Technical Conference and Exposition, American Society of Mechanical Engineers, 2018, p. V003T08A002.

[15] F. Alobaid, R. Postler, J. Ströhle, B. Epple, H.-G. Kim, Modeling and investigation start-up procedures of a combined cycle power plant, Appl. Energy 85 (12) (2008) 1173–1189.

[16] T. Kim, D. Lee, S. Ro, Analysis of thermal stress evolution in the steam drum during start-up of a heat recovery steam generator, Appl. Therm. Eng. 20 (11) (2000) 977–992.

[17] S.C. Gülen, K. Kim, Gas turbine combined cycle dynamic simulation: a physics based simple approach, J. Eng. Gas Turbines Power 136 (1) (2014) 011601.

[18] P. Dzierwa, J. Taler, Optimum heating of pressure vessels with holes, J. Pressure Vessel Technol. 137 (1) (2015) 011202.

[19] J. Taler, P. Dzierwa, D. Taler, P. Harchut, Optimization of the boiler start-up taking into account thermal stresses, Energy 92 (2015) 160–170.

[20] J. Taler, B. Weglowski, D. Taler, T. Sobota, P. Dzierwa, M. Trojan, P. Madejski, M. Pilarczyk, Determination of start-up curves for a boiler with natural circulation based on the analysis of stress distribution in critical pressure components, Energy 92 (2015) 153–159.

[21] J. Bausa, G. Tsatsaronis, Dynamic optimization of startup and load-increasing processes in power plants – Part I: Method, J. Eng. Gas Turbines Power 123 (1) (2001) 246–250.

[22] T. Akiyama, H. Matsumoto, K. Asakura, Dynamic simulation and its applications to optimum operation support for advanced combined cycle plants, Energy Convers. Manage. 38 (15–17) (1997) 1709–1723.

[23] H. Matsumoto, Y. Ohsawa, S. Takahasi, T. Akiyama, H. Hanaoka, O. Ishiguro, Startup optimization of a combined cycle power plant based on cooperative fuzzy reasoning and a neural network, IEEE Trans. Energy Convers. 12 (1) (1997) 51–59.

[24] M. Shirakawa, M. Nakamoto, S. Hosaka, Dynamic simulation and optimization of start-up processes in combined cycle power plants, JSME Int. J. Ser. B Fluids Therm. Eng. 48 (1) (2005) 122–128.

[25] C. Albanesi, M. Bossi, L. Magni, J. Paderno, F. Pretolani, P. Kuehl, M. Diehl, Optimization of the start-up procedure of a combined cycle power plant, in: 2006 45th IEEE Conference on Decision and Control, IEEE, 2006, pp. 1840–1845.

[26] F. Casella, F. Pretolani, Fast start-up of a combined cycle power plant: a simulation study with modelica, 5th International Modelica Conference, Vienna, Austria, September, 2006, pp. 3–10.

[27] J. Bausa, G. Tsatsaronis, Dynamic optimization of startup and load-increasing processes in power plants – Part II: Application, J. Eng. Gas Turbines Power 123 (1) (2001) 251–254.

[28] G. Prasad, E. Swidenbank, B. Hogg, A local model networks based multivariable long-range predictive control strategy for thermal power plants, Automatica 34 (10) (1998) 1185–1204.

[29] G. Prasad, E. Swidenbank, B. Hogg, A neural net model-based multivariable long-range predictive control strategy applied in thermal power plant control, IEEE Trans. Energy Convers. 13 (2) (1998) 176–182.

[30] H. Peng, J. Wu, G. Inoussa, Q. Deng, K. Nakano, Nonlinear system modeling and predictive control using the RBF nets-based quasi-linear ARX model, Control Eng. Pract. 17 (1) (2009) 59–66.

[31] H. Peng, T. Ozaki, Y. Toyoda, K. Oda, Exponential ARX model-based long-range predictive control strategy for power plants, Control Eng. Pract. 9 (12) (2001) 1353–1360.

[32] S. Lu, B.W. Hogg, Predictive co-ordinated control for power-plant steam pressure and power output, Control Eng. Pract. 5 (1) (1997) 79–84.

[33] F.J. D'Amato, Industrial application of a model predictive control solution for power plant startups, in: Computer Aided Control System Design, 2006 IEEE International Conference on Control Applications, 2006 IEEE International Symposium on Intelligent Control, 2006 IEEE, IEEE, 2006, pp. 243–248.

[34] P. Sindareh-Esfahani, S.S. Tabatabaei, J.K. Pieper, Model predictive control of a heat recovery steam generator during cold start-up operation using piecewise linear models, Appl. Therm. Eng. 119 (2017) 516–529.

[35] R. Viswanathan, J. Stringer, Failure mechanisms of high temperature components in power plants, J. Eng. Mater. Technol. 122 (3) (2000) 246–255.

[36] S. Barella, M. Bellogini, M. Boniardi, S. Cincera, Failure analysis of a steam turbine rotor, Eng. Fail. Anal. 18 (6) (2011) 1511–1519.

[37] A. Mirandola, A. Stoppato, E.L. Casto, Evaluation of the effects of the operation strategy of a steam power plant on the residual life of its devices, Energy 35 (2) (2010) 1024–1032.

[38] A. Benato, A. Stoppato, S. Bracco, Combined cycle power plants: a comparison between two different dynamic models to evaluate transient behaviour and residual life, Energy Convers. Manage. 87 (2014) 1269–1280.

[39] Thermoflow Inc, GT PRO 24.0, 2014.

[40] Modelon, Thermal Power Library. https://www.modelon.com/library/thermal-power-library/.

[41] Dassault Systemes. https://www.3ds.com/products-services/catia/products/ dymola/.

[42] Modelica Association. https://www.modelica.org/.

[43] R.M. Montañés, S.Ó. GarDarsdóttir, F. Normann, F. Johnsson, L.O. Nord, Demonstrating load-change transient performance of a commercial-scale natural gas combined cycle power plant with post-combustion CO_2 capture, Int. J. Greenhouse Gas Control 63 (2017) 158–174.

[44] L. Ljung, System Identification: Theory for the User, Prentice-hall, 1987.

[45] T.A. Johansen, B. Foss, Constructing NARMAX models using ARMAX models, Int. J. Control 58 (5) (1993) 1125–1153.

[46] M. Gevers, Identification for control: from the early achievements to the revival of experiment design, Eur. J. Control 11 (2005) 1–18.

[47] M. Gevers, L. Ljung, Optimal experiment designs with respect to the intended model application, Automatica 22 (5) (1986) 543–554.

[48] U. Forssell, L. Ljung, Closed-loop identification revisited, Automatica 35 (7) (1999) 1215–1241.

[49] L. Mišković, A. Karimi, D. Bonvin, M. Gevers, Closed-loop identification of multi-variable systems: with or without excitation of all references? Automatica 44 (8) (2008) 2048–2056.

[50] M. Gevers, L. Mišković, D. Bonvin, A. Karimi, Identification of multi-input systems: variance analysis and input design issues, Automatica 42 (4) (2006) 559–572.

[51] S. Timoshenko, J.N. Goodier, Theory of Elasticity, McGraw-Hill book Company, 1951.

[52] Mathworks Inc, MATLAB version R2018a, 2018.

[53] ANSYS, ANSYS Academic Research Thermal and Mechanical, Release 19.2, ANSYS Inc, 2018.

[54] R. Kehlhofer, F. Hannemann, B. Rukes, F. Stirnimann, Combined-cycle Gas & Steam Turbine Power Plants, Pennwell Books, 2009.

[55] P.J. Dechamps, Modelling the transient behaviour of heat recovery steam generators, Proc. Inst. Mech. Eng., Part A: J. Power Energy 209 (4) (1995) 265–273.

[56] K. Jonshagen, M. Genrup, Improved load control for a steam cycle combined heat and power plant, Energy 35 (4) (2010) 1694–1700.

[57] J. Nocedal, S.J. Wright, Numerical Optimization, Springer, 2006.

[58] R. Viswanathan, W. Bakker, Materials for ultrasupercritical coal power plants - Turbine materials: Part II, J. Mater. Eng. Perform. 10 (1) (2001) 96–101.